Subharmonic gap structures and Josephson effect in MgB$_2$/Nb microconstrictions

F. Giubileo,[1,*] M. Aprili,[2] F. Bobba,[1] S. Piano,[1] A. Scarfato,[1] and A. M. Cucolo[1]

[1]*Physics Department and CNR-SUPERMAT Laboratory, University of Salerno, Via S. Allende, 84081 Baronissi (SA), Italy*
[2]*Laboratoire de Spectroscopie en Lumière Polarisée, ESPCI, 10 rue Vauquelin, 75005 Paris, France
and CSNSM-CNRS, Bat. 108 Université Paris-Sud, 91405 Orsay, France*

Superconducting microconstrictions between Nb tips and high-quality MgB$_2$ pellets have been realized by means of a point-contact inset, driven by a micrometric screw. Measurements of the current-voltage characteristics and of the dynamical conductance versus bias have been performed in the temperature range between 4.2 K and 500 K. Above the Nb critical temperature T_C^{Nb}, the conductance of the MgB$_2$/normal-metal constrictions behaves as predicted by the Blonder-Tinkham-Klapwijk model for low-resistance contacts while high-resistance junctions show quasiparticle tunneling characteristics. Consistently, from the whole set of data we infer the value $\Delta_\pi = 2.5 \pm 0.2$ meV for the three-dimensional (3D) gap of MgB$_2$. Below T_C^{Nb}, low-resistance contacts show Josephson current and subharmonic gap structures, due to multiple Andreev reflections. Simultaneous observations of both features unambiguously indicate a coupling of the 3D band of MgB$_2$ with the Nb superconducting order parameter. We found that the temperature dependence of the Josephson critical current follows the classical Ambegaokar-Baratoff behavior with a value $I_C R_N = (2.1 \pm 0.1)$ meV at low temperatures.

I. INTRODUCTION

The discovery of superconductivity in the binary intermetallic MgB$_2$ compound[1] has given rise to a considerable effort in the condensed matter community in the last years. Besides the great interest in understanding the new physics originating from the multiband nature of this material, attention has been paid to the attractive potential applications in superconducting electronics, because of the remarkably high critical temperature ($T_C \simeq 39$ K) simple crystal structure, relatively long coherence lengths[2] ($\xi^c \simeq 25$ Å, $\xi^{ab} \simeq 65$ Å), and low surface resistance[3] ($R_S \simeq 0.8$ mΩ at $T = 24$ K).

From the structural point of view, the intermetallic MgB$_2$ superconductor is very similar to graphite with the crystal lattice formed by honeycomb layers of B atoms intercalated by layers of Mg atoms, sitting at the center of each underlying hexagon. From the theoretical point of view, this compound presents a rare example of two disconnected parts of the Fermi surface: a two-dimensional (2D) hole-type σ band and a three-dimensional (3D) electron-type π band.[4,5] The unusual consequence of this band structure makes it such that in the clean limit[6] two different energy gaps are formed at the Fermi level, both closing at the same temperature T_C. Indeed, two superconducting energy gaps have been experimentally observed by different techniques, including tunneling spectroscopy,[7–15] specific heat measurements,[16,17] Raman spectroscopy,[18,19] and high-resolution photoemission.[20] The majority of these studies agree with the presence of a larger gap around $\Delta_\sigma = 7.0 - 7.5$ meV attributed to the 2D σ band and a smaller gap $\Delta_\pi = 2.0 - 2.8$ meV due to the 3D π band. In the dirty limit a large amount of impurity scattering causes the two gaps to merge to an intermediate value $\Delta_D \simeq 4.1$ meV, which closes at a reduced T_C.[21,22]

The physics of multiband superconductors has been intensively studied since the appearance of the original theoretical works,[6,21,23] and different phenomena are expected due to the presence of different condensates in the same material. The predictions have been tested in few cases, such as, e.g., in niobium-doped SrTiO$_3$ (Ref. 24) or in nickel borocarbides (Ref. 25). Due to these considerations, MgB$_2$ appeared, from the beginning, as a natural candidate to investigate the peculiarities of a two-band superconductor. Recently, a multiband model for quasiparticle and Josephson tunneling in MgB$_2$-based junctions has been developed.[21] Depending on the different bands exposed at the sides of the insulating barrier, different temperature behaviors of the Josephson current have been predicted with values of the $I_C R_N$ product at low temperatures as high as 9.9 mV and 5.9 mV for tunneling along the a-b planes and c direction, respectively. In the experiments, however, effective Josephson coupling of the 2D band σ with a 3D band, both of a MgB$_2$ or of a conventional superconducting counterelectrode, has been not observed. In addition to this, the measured $I_C R_N$ values are often severely depressed, and regardless of the junction orientation, different temperature dependences of the Josephson current are often reported.[12,14,26–29] Similar behavior is expected in proximity-coupled S-I-N-S structures,[30] and in MgB$_2$ junctions it has been attributed to degradation of T_C at the interface and/or to the barrier nature and quality.

Besides the analysis of the Josephson coupling, the study of subharmonic gap structures (SGS's) at voltages less than Δ is itself interesting. These resonances, due to the coupling of the gap functions at the sides of the barrier, have been mainly studied in symmetric S-I-S junctions.[31–39] In this case, conductance enhancements appearing at voltages $V_n = 2\Delta/n (n = 1, 2, 3, \ldots)$ have been observed.[40–45] In junctions with dissimilar superconductors (S-I-S') conductance structures appear at energies $(\Delta_S + \Delta_{S'})/m$ (with $m = 1, 3, 5, \ldots$), $\Delta_{S'}/n$, and Δ_S/n (with $n = 1, 2, 3, \ldots$), depending on the energy ratio $\Delta_{S'}/\Delta_S$.[46,47]

In this paper we address the problem of the behavior of both SGS's and Josephson current in a multiband supercon-

ductor. Since both phenomena depend on the multiplicity of the order parameter in the two electrodes, the simultaneous presence of SGS's and Josephson effect allows a consistent cross-check to verify the effective coupling of different condensates at the sides of the tunnel barrier. To investigate this aspect more deeply, we have realized point-contact (PC) junctions between MgB_2 pellets and Nb tips. The aim of our study was to check for the Josephson coupling of the Nb order parameter with both the 2D and/or 3D MgB_2 bands, this aspect being reinforced by the appearance of the related subharmonic gap resonances. In the following we report, to the best of our knowledge, the first detailed study of the temperature dependence of both subharmonic gap structures and Josephson current observed in asymmetric Nb-MgB_2 microconstrictions. Current-voltage characteristics (I-V) and conductance spectra (dI/dV vs V) were measured by using a homebuilt point-contact apparatus, in which a Nb tip was pressed into high-quality MgB_2 pellets, to favor the possible interaction with both bands of this compound.

II. SUPERCONDUCTING CONTACTS

A point-contact junction between a superconductor and a normal metal (SN contact) or between two superconductors (SS′ contact) is a convenient geometry to study different aspects of superconductivity. Indeed, the possibility of varying the strength of the potential barrier, as well as of changing the contact area between the electrodes, allows the observation of a large number of phenomena by realizing a continuous variation from a metallic contact N-c-S (c is the constriction) to a tunnel junction N-I-S (I is the insulating barrier). This transition has been theoretically and experimentally studied by Blonder, Tinkham, and Klapwijk[48] (BTK) within a generalized semiconductor model using the Bogoliubov equations to treat the transmission and reflection of quasiparticles at the interface. For a conventional BCS superconductor, there are two parameters in the model that are varied to reproduce the conductance curves: the superconducting energy gap Δ and a dimensionless parameter Z taking into account the barrier strength.

SN metallic contacts with low barriers ($Z \to 0$) show enhanced current at bias voltages less than the superconducting energy gap because Andreev reflections are the dominant transport process at the interface.[48] In this case, an incoming electron from the normal metal with energy $E < \Delta$ cannot enter in the superconducting electrode and is reflected as a hole in the normal metal, simultaneously adding a Cooper pair to the condensate in the superconductor [Fig. 1(a)]. This process causes an increase of the conductance around zero bias with a maximum ratio of $G(V=0)/G_N(V \gg \Delta) = 2$. On the other hand, in the tunneling regime ($Z \to \infty$), the probability of Andreev reflections is negligible and the BTK model yields a conductance characteristic that, at low temperatures for conventional superconductors, directly reproduces the BCS superconducting density of states at the Fermi level. In the intermediate case, both tunneling and Andreev reflections contribute to the transport through the barrier [Fig. 1(b)].

A different situation is realized when both electrodes forming the microconstriction are superconducting. The
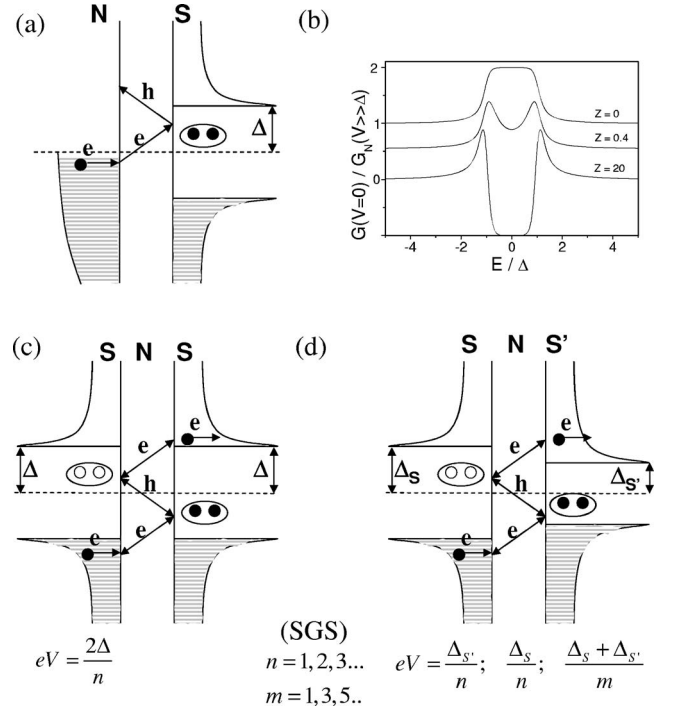

FIG. 1. (a) An electron coming from the normal electrode with energy smaller than the energy gap cannot enter the superconductor. It is reflected as a hole, leaving an extra charge $2e$ in the superconducting condensate (Andreev reflection). At low temperatures, the conductance spectra depend on the barrier strength Z, as shown in (b). The scale refers to the curve for $Z=0$; the other curves are shifted for clarity. In the case of superconducting electrodes (c), an electron is reflected back or transmitted. For voltages $eV \lesssim \Delta$ the Andreev-reflected hole cannot find an empty state in the left electrode but is Andreev reflected in turn as an electron. For energies $2\Delta/3 \lesssim eV < \Delta/2$ the electron finds an empty state in the right electrode; three charges are transferred in this process [multiple Andreev reflections (MAR's)]. For smaller voltages, MAR processes that transfer four or more electron charges carry the current. (d) In asymmetric tunnel junctions the conductance enhancements appear at energies $(\Delta_S + \Delta_{S'})/m$, with $m = 1, 3, 5, \ldots$, and Δ_S/n and $\Delta_{S'}/n$, with $n = 1, 2, 3, \ldots$.

main features in the current voltage characteristics of such junctions are the presence of Josephson current and SGS. In particular, these last features have been observed in junctions between identical superconductors as conductance peaks appearing at bias voltages $V = 2\Delta/ne$ with $n = 1, 2, 3, \ldots$.[41,42,44] Different mechanisms have been suggested to describe this phenomenon: initially, the correctly multiparticle tunneling model[49] (MPT) was able to predict the voltage positions of the SGS. Successively, a satisfactory explanation of the subgap structures has been proposed in the BTK theory[48] and then extended in the Octavio-Tinkham-Blonder-Klapwijk (OBTK) model by Octavio *et al.*:[37] SGS's are originating from multiple Andreev reflections at the superconductor-normal-metal interfaces; see Fig. 1(c). This model has been then generalized by Arnold[38] to any kind of junctions between two superconductors and in particular to the superconducting point contacts by using a modified tunneling Hamiltonian approach. It is now understood that MPT model

represents the low-transparency perturbation theory limit of the more general process of MAR's.[39]

Unlike symmetric junctions, very few reports in the literature address the behavior of asymmetric S-c-S′ constrictions [see Fig. 1(d)], both theoretically[37,47] and experimentally.[40,46] In particular, calculation of the current-voltage relations for ballistic S-N-S′ junctions by means of transmission formalism[47] showed that, for finite temperatures, SGS's appear in the differential conductance at energies $eV_n = (\Delta_S + \Delta_{S'})/m$, with $m = 1, 3, 5, \ldots$, and $eV_n = \Delta_S/n$ and $eV_n = \Delta_{S'}/n$, with $n = 1, 2, 3, \ldots$.

III. CONDUCTANCE CHARACTERISTICS FOR $T > T_C^{Nb}$

The polycrystalline MgB_2 pellets used in the present work showed resistive superconducting transitions at $T_C(\rho = 0) = 38.8$ K, with $\Delta T_C \simeq 0.5$ K. The sample surface was chemically etched in a 1% HCl solution in pure ethanol. The Nb tips were prepared by cutting a thin (0.2 mm) Nb wire and then treated by electrochemical etching. Soon after, the PC inset was placed in liquid ^{4}He to limit surface degradation effects. The contacts were established by driving the Nb tip into the sample surface at low temperatures. The vertical movement of the tip, driven by a micrometric screw with a precision of about 0.1 μm, allowed the tuning of the contact resistance from tunneling regime to metallic contact. Our experimental setup resulted in being extremely stable, showing no relevant effects of thermal contraction, so that in many cases it was possible to vary the junction temperature without affecting the contact geometry.

All measurements were performed in the temperature range between 4.2 K and 50 K. Current and dI/dV versus V characteristics were measured by using a standard four-probe method and a lock-in technique by superimposing a small ac modulation to a slowly varying bias voltage. Each measurement comprises two successive cycles in order to check for the absence of heating hysteresis effects.[50,51]

In Figs. 2(b) and 2(c) we show the conductance spectra measured for high and low junction resistances above the niobium critical temperature T_C^{Nb}. These are representative of several measurements carried out on different contacts. The rich variety of our experimental spectra shows the versatility of the point-contact technique in modulating the barrier strength of the established junctions. High contact resistances were obtained by pushing the Nb tip into the MgB_2 and then slightly releasing the pressure. In this case, the conductance curves show typical tunneling behavior, Fig. 2(b). The temperature dependence of the zero-bias tunneling conductance, reported in the inset, suggests that rather than a S-I-N junction, the contact is formed between two MgB_2 grains. Indeed, a zero-bias conductance peak is found as for S-I-S junctions, due to thermally activated quasiparticles with spectral weight increasing for rising temperatures. The S-I-S behavior has been observed in other experiments of point contact spectroscopy in polycrystalline HTC superconductors,[9,52] and it has been attributed to a small piece of the base electrode captured by the tip apex. Due to the granularity of the samples, also in our case when releasing the pressure, one MgB_2 grain remains on the Nb tip; see
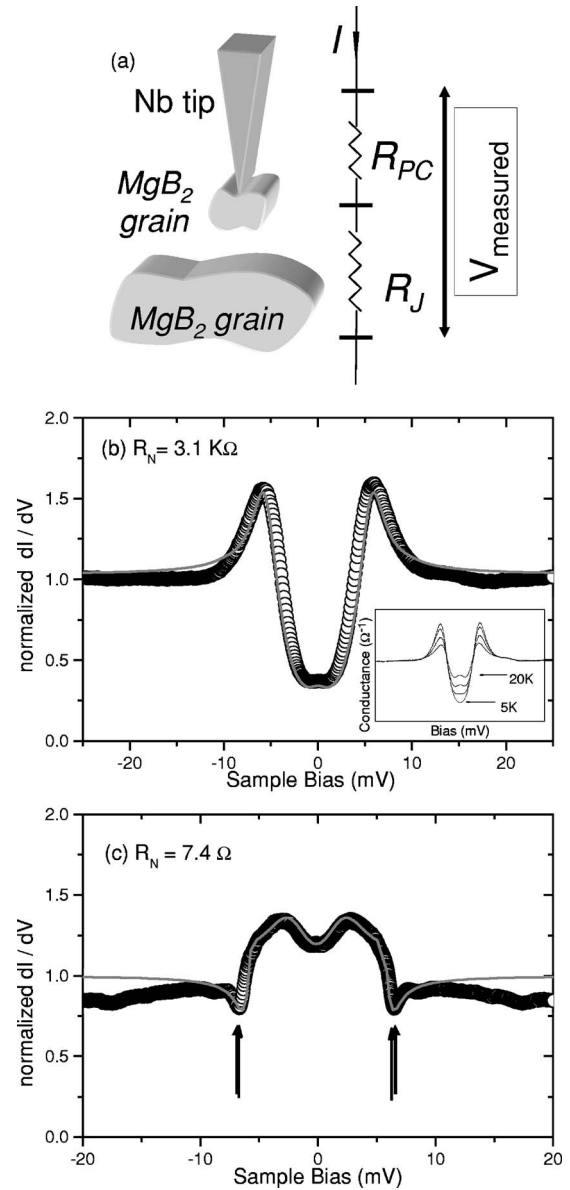

FIG. 2. (a) A small MgB_2 grain remains on the Nb tip realizing two junctions in series: the point contact between the Nb tip and the small grain with resistance R_{PC} and the Josephson junction between the two MgB_2 grains with resistance R_J. The measured voltage V_{meas} is the sum of the voltage drops at both junctions. (b) Tunneling conductance for a high-resistance contact measured at $T = 12$ K. Experimental data (scattered graph) are compared to the theoretical simulation (solid line) for a S-I-S tunnel junction between two MgB_2 with $\Delta_\pi = 2.7$ meV and $\Gamma = 0.7$ meV. (c) Conductance spectrum at $T = 12$ K for a low-resistance contact. The theoretical simulation (solid line) has been obtained with $\Delta_\pi = 2.4$ meV, $Z = 0.66$, and $\Gamma = 0$ considering the formation of an intergrain MgB_2/MgB_2 junction in series with $R_J = 1.5$ Ω and $I_J = 1.2$ mA.

Fig. 2(a). Two junctions in series are so formed, and in the analysis of the data attention has to be payed to the relative weight of the related junction resistances. In the tunneling regime, the contribution of the point-contact junction is not critical, since $R_{PC} \ll R_J$. On the other hand, this has to be

taken into account, in the point-contact regime, with both resistances of the same order of magnitude. The tunneling conductance characteristics, measured at $T=12$ K [scattered graph in Fig. 2(b)], were so compared to the theoretical fitting for a S-I-S tunnel junction between two identical superconductors (solid line). Since $R_N=3.1$ kΩ, we did not consider the contribution of the point contact in series. $\Delta_\pi = 2.7$ meV was used in the fitting in which a broadening parameter, representative of the quasiparticle finite lifetime $\Gamma = 0.7$ meV, was also included.[53]

The conductance spectrum of a low-resistance contact is shown in Fig. 2(c), where the expected Andreev reflection behavior with conductance enhancement for $eV < \Delta$ is observed. The conductance characteristic also shows dip structures at energies higher than the AR feature (arrows in the figure), which are not reproduced by the usual BTK theory. The origin of these dips has been related to proximity effect[54] and/or to the formation of a junction in series.[55] In our case, for a satisfactory fitting of the experimental data, it was necessary to consider a more complex configuration, consistent with the assumption shown in Fig. 2(a). Indeed, when the resistance of the point-contact junction (R_{PC}) is comparable with the resistance of the Josephson junction (R_J), we have to consider the formation of two junctions in series: the SN point contact between the Nb tip and MgB$_2$ and the intergrain, low-resistance MgB$_2$/MgB$_2$ junction. As shown in Fig. 2(a), as the PC tip/grain junction is approached to the base MgB$_2$ electrode, the latter junction reduces its resistance, and the two MgB$_2$ grains can be coupled by Josephson effect. The measured voltage is now given by the sum of two contributions—i.e., the voltage drop V_{PC} at the point contact and V_J at the Josephson junction. In the limit of small capacitance C, the average contribution V_J can be simulated by the modified resistively shunted junction model given by Lee,[56] where

$$\langle V_J \rangle = \frac{2}{\gamma} R_J I_J \frac{\exp(\pi\gamma\alpha) - 1}{\exp(\pi\gamma\alpha)} T_2^{-1}, \tag{1}$$

with $\alpha = I/I_J$ the normalized current, I_J the Josephson current of the junction in series, $\gamma = hI_J/eK_BT_n$ (T_n being the effective noise temperature), and

$$T_2 = \int_0^{2\pi} d\varphi \sin\frac{\varphi}{2} I_1\left(\gamma \sin\frac{\varphi}{2}\right) \exp\left[-\left(\frac{\gamma}{2}\alpha\right)\varphi\right],$$

where $I_1(x)$ is the modified Bessel function. The conductance $\sigma(V)$ is then calculated by the formula

$$\sigma(V) = dI/dV = (dV_{PC}/dI + dV_J/dI)^{-1}, \tag{2}$$

where the PC contribution is simulated by the usual BTK model. The best theoretical fitting [solid line in Fig. 2(c)], reproducing also the side dips, was obtained for $\Delta_\pi = 2.4$ meV and $Z=0.66$, and no smearing factor Γ was needed for this junction.

We notice that the presence of the Josephson junction in series introduces in the model two more fitting parameters, the resistance $R_J = 1.5$ Ω and the critical current $I_J = 1.2$ mA of the Josephson junction; these, however, are not independent one from the other and from the measured resistance.

We remark here that, since the measured voltage $V_{meas} = V_{PC} + V_J > V_{PC}$, a theoretical fitting that did not take into account the presence of the additional V_J would give an overestimation of the MgB$_2$ superconducting energy gap.[57,58] From our discussion, it appears that PC spectroscopy reveals two types of junctions depending on the contact resistance: MgB$_2$/MgB$_2$ at high resistances when the tip/grain junction is left far from the surface and MgB$_2$/Nb at low resistances when the tip/grain junction is pushed into the surface. From the whole set of data at $T > T_C^{Nb}$, obtained in several locations, we have found, as the average value of the 3D gap, $\Delta_\pi = 2.5 \pm 0.2$ meV.

IV. CONDUCTANCE CHARACTERISTICS FOR $T < T_C^{Nb}$

As we already mentioned, the analysis of the Josephson coupling between a two-band superconductor and a conventional one has been relatively less studied in the literature with contradictory results about both the values of the $I_C R_N$ product and its temperature dependence. In comparison with the theoretical predictions,[21] the majority of the reports indicate depressed values of such a product and different temperature behaviors irrespectively of the weak link or tunnel nature of the junctions.[12,14,26,28,29] To the best of our knowledge, in the majority of the cases coupling of the conventional superconductor with only the 3D band of the multigap material is inferred.

In this section we analyze the conductance data of low-resistance junctions for $T < T_C^{Nb}$ in which both Josephson effect and subharmonic gap structures appear. Indeed, the simultaneous presence of these features makes unambiguous any conclusion about the coupling between the Nb order parameter and the 2D or 3D band of MgB$_2$. In addition to this, the study of the behavior of the subgap features in asymmetric junctions is itself of interest, since few reports can be found in the literature.

In Figs. 3(a) and 3(b) we show the conductance spectra measured at $T=7$ K for two different contacts. The spectra are characterized by the huge conductance peak at zero bias, the signature of the Josephson current flowing through the electrodes, as confirmed by the corresponding I-V characteristics shown in the insets. In addition to this, subharmonic gap structures at low energies appear in both cases. Similar structures have been seldomly observed in MgB$_2$ junctions; however, a detailed analysis of their origin and/or temperature dependence was not carried out.[9,59]

In Fig. 3 we identify three principal features for junction (a), localized at energies $E_1 \simeq \pm 1.2$ meV, $E_2 \simeq \pm 2.4$ meV, and $E_3 \simeq \pm 3.5$ meV, while only E_1 and E_3 are visible in junction (b), at the same energies. As discussed above, these structures can be explained in terms of multiple Andreev reflections that enhance conductance at voltages Δ_1/n, Δ_2/n, and $(\Delta_1 + \Delta_2)$. The most useful way to identify the origin of various SGS's can be obtained by studying their temperature dependence. Due to the high stability of our system, the dynamical conductance of both the contacts was measured in the temperature range between 4.2 K and 12 K. Since the two superconductors have quite different critical temperatures ($T_C^{MgB_2} \simeq 39$ K and $T_C^{Nb} \simeq 9.2$ K) for these temperatures,
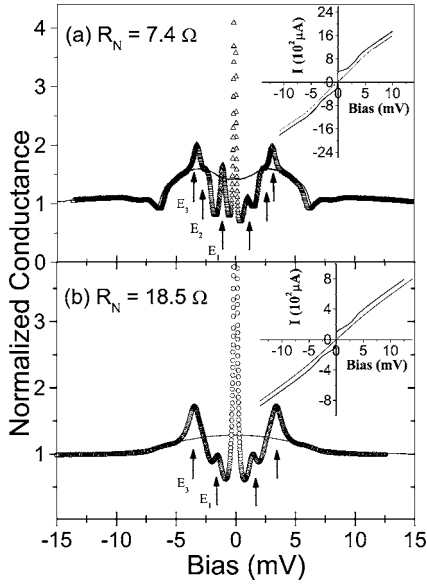
FIG. 3. Conductance spectra for two different contacts measured at $T=7$ K (scattered graphs). The conductance measured at $T=12$ K—i.e., above T_C^{Nb}—is also reported (solid lines). The arrows indicate the energies of the SGS's. Insets: current-voltage characteristics of the same junctions.

only changes in the Nb energy gap are expected to affect the evolution of the SGS.

In Fig. 4(a) we show the temperature dependence of the conductance spectra for the junction of Fig. 3(a). We clearly see that the feature at the highest energy (E_3) changes in temperature while $E_2 \simeq \pm 2.4$ mV and $E_1 \simeq \pm 1.2$ mV remain quite stable, suggesting that these are related to MgB$_2$. In

Fig. 4(b), we report the temperature dependence of the energy positions of the SGS for both junctions of Fig. 3, with solid and open symbols referring to junctions (a) and (b), respectively. Due to the fact that all the structures appear for voltages lower than 3.0 mV, we exclude the influence of the 2D σ band in the formation of the resonances. We then make the following identification: $E_3 \to \Delta_\pi^{MgB_2} + \Delta^{Nb}$, $E_2 \to \Delta_\pi^{MgB_2}$, and $E_1 \to \Delta_\pi^{MgB_2}/2$, consistently with the MgB$_2$ value of $\Delta_\pi = 2.4$ meV inferred from the theoretical fitting of the data at $T > T_C^{Nb}$ [Fig. 3(c)]. To confirm our hypothesis, we have extracted the temperature dependence of the Nb gap from the data $E_3(T)$ and $E_2(T)$, being $\Delta^{Nb}(T) = E_3(T) - E_2(T)$. The result is plotted in Fig. 4(c) where the experimental data correctly follow the theoretical behavior (solid line) expected for the Nb energy gap. In particular, the theoretical fitting gives $\Delta^{Nb}(T=0) = 1.4$ meV and a local critical temperature $T_C^{Nb} = 9.2$ K. We notice that the E_2 structure only appears in the lower-resistance junction [Fig. 3(a)], and its amplitude is relatively depressed in comparison with E_1 and E_3. Indeed, for this contact, we measured a higher value of the Josephson current which, in comparison with junction (b), implies a stronger coupling between the two electrodes.

In Fig. 5, we finally report the $I_C R_N$ product versus temperature for both contacts in Figs. 3(a) and 3(b). $I_C = 290$ μA and $I_C = 110$ μA were measured in these junctions with $R_N = 7.4$ Ω and $R_N = 18.5$ Ω, respectively. This implies $I_C R_N = (2.1 \pm 0.1)$ mV at $T = 4.5$ K, among the highest values reported in the literature.[12,14,27] Our values are very close to those predicted when the superconducting Nb couples with the MgB$_2$ π band[21] and follow the expected Ambegaokar-Baratoff temperature behavior.[21,30] From our discussion it unambiguously appears that coupling of the Nb energy gap only occurs with the MgB$_2$ 3D Δ_π band, while in more than
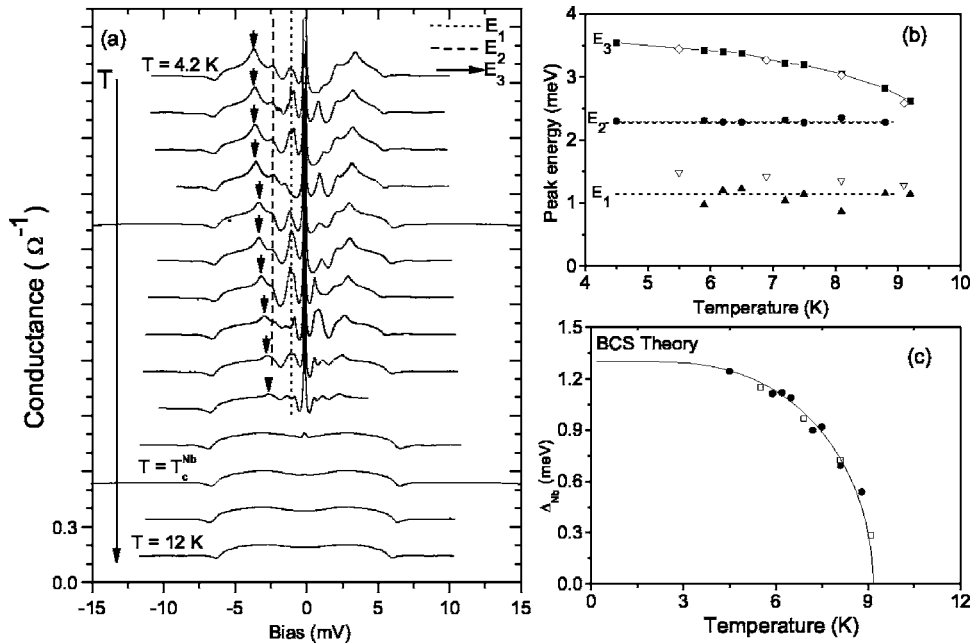

FIG. 4. (a) Temperature dependence of the conductance spectra of the junction in Fig. 3(a) in the range between 4.2 K and 12 K. All the spectra have been shifted, and the scale is valid only for the highest-temperature data. The arrows indicate the energy positions of the E_3 feature. (b) Temperature dependence of E_1, E_2, and E_3. Dotted and solid lines are guidelines for the eye. Open symbols correspond to sample in Fig. 3(b). (c) Temperature dependence of $\Delta^{Nb}(T) = E_3(T) - E_2(T)$ (symbols) and theoretical curve (solid line).
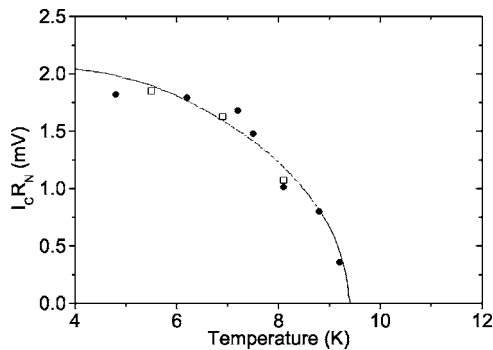
FIG. 5. Temperature dependence of the $I_C R_N$ product. The experimental data (scattered graph) are compared to the Ambegaokar-Baratoff behavior (solid line).

50 measured contacts we never found evidence for coupling with the 2D Δ_σ band. We have also demonstrated that it is in principle possible to avoid the MgB$_2$-degraded surface layer, responsible for both depressed values of the $I_C R_N$ product and nonconventional temperature behavior.

V. CONCLUSION

We have realized superconducting microconstrictions between high-quality MgB$_2$ pellets and electrochemically etched Nb tips. The conductance as a function of bias measured above the Nb critical temperature reveals that an inter-

grain MgB$_2$/MgB$_2$ junction is often formed in series with the MgB$_2$/Nb contact. This results from a small piece of MgB$_2$ remaining on the tip apex when relieved from the pellet. Depending on the tip pressure the MgB$_2$/MgB$_2$ contact resistance can be either larger (tip far from the pellet) or comparable (tip into the pellet) with the MgB$_2$/Nb point-contact resistance. In the last case, an accurate theoretical analysis has to be carried out to extract the correct value of the MgB$_2$ superconducting energy gap. For $T < T_C^{Nb}$, we have observed the Josephson effect as well as subgap resonances. We explain these features in terms of subharmonic gap structures due to multiple Andreev reflections. From the analysis of the SGS, consistently with the values measured for $T > T_C^{Nb}$, we have extracted the correct temperature dependence of the Nb energy gap and the value $\Delta_\pi \simeq 2.4$ meV for the 3D energy gap at the MgB$_2$ Fermi surface. In our junctions, at $T = 4.5$ K, we have measured $I_C R_N$ values up to 2.2 meV, among the highest reported in the literature. The temperature dependence of the $I_C R_N$ product follows the classical Ambegaokar-Baratoff behavior. Both observations completely confirm the results predicted by a recent theoretical model.[21] In addition to this, the simultaneous observation of both Josephson current and SGS's unambiguously indicates the coupling of the Nb energy gap with the MgB$_2$ 3D band.

ACKNOWLEDGMENT

*Electronic address: giubileo@sa.infn.it

[1] J. Nagamatsu, N. Nakagawa, T. Muranaka, Y. Zenitani, and J. Akimitsu, Nature (London) **410**, 63 (2001).

[2] M. Xu, H. Kitazawa, Y. Takano, J. Ye, K. Nishida, H. Abe, A. Matsushita, N. Tsujii, and G. Kido, Appl. Phys. Lett. **79**, 2779 (2001).

[3] S. Y. Lee, J. H. Lee, J. S. Ryu, J. Lim, S. H. Moon, H. N. Lee, H. G. Kim, and B. Oh, Appl. Phys. Lett. **79**, 3299 (2001).

[4] J. Kortus, I. I. Mazin, K. D. Belashchenko, V. P. Antropov, and L. L. Boyer, Phys. Rev. Lett. **86**, 4656 (2001).

[5] S. V. Shulga, S.-L. Drechsler, H. Eshrig, H. Rosner, and W. E. Pickett, cond-mat/0103154 (unpublished).

[6] A. Y. Liu, I. I. Mazin, and J. Kortus, Phys. Rev. Lett. **87**, 087005 (2001).

[7] F. Giubileo, D. Roditchev, W. Sacks, R. Lamy, D. X. Thanh, J. Klein, S. Miraglia, D. Fruchart, J. Marcus, and P. Monod, Phys. Rev. Lett. **87**, 177008 (2001).

[8] M. Iavarone, G. Karapetrov, A. E. Koshelev, W. K. Kwok, G. W. Crabtree, D. G. Hinks, W. N. Kang, E.-M. Choi, H. J. Kim, H.-J. Kim, and S. I. Lee, Phys. Rev. Lett. **89**, 187002 (2002).

[9] P. Martinez-Samper, J. G. Rodrigo, G. Rubio-Bollinger, H. Suderow, S. Vieira, S. Lee, and S. Tajima, Physica C **385**, 233 (2002).

[10] P. Szabó, P. Samuely, J. Kacmarcík, T. Klein, J. Marcus, D. Fruchart, S. Miraglia, C. Marcenat, and A. G. M. Jansen, Phys. Rev. Lett. **87**, 137005 (2001).

[11] Y. Bugoslavsky, Y. Miyoshi, G. K. Perkins, A. V. Berenov, Z. Lockman, J. L. MacManus-Driscoll, L. F. Cohen, A. D. Caplin, H. Y. Zhai, M. P. Paranthaman, H. M. Christen, and M. Blamire, Supercond. Sci. Technol. **15**, 526 (2002).

[12] R. S. Gonnelli, A. Calzolari, D. Daghero, G. A. Ummarino, V. A. Stepanov, G. Giunchi, S. Ceresara, and G. Ripamonti, Phys. Rev. Lett. **87**, 097001 (2001).

[13] H. Schmidt, J. F. Zasadzinski, K. E. Gray, and D. G. Hinks, Phys. Rev. Lett. **88**, 127002 (2002).

[14] G. Carapella, N. Martucciello, G. Costabile, C. Ferdeghini, V. Ferrando, and G. Grassano, Appl. Phys. Lett. **80**, 2949 (2002).

[15] M. H. Badr, M. Freamat, Y. Sushko, and K.-W. Ng, Phys. Rev. B **65**, 184516 (2002).

[16] Y. Wang, T. Plackowski, and A. Junod, Physica C **355**, 179 (2001).

[17] F. Bouquet, R. A. Fisher, N. E. Phillips, D. G. Hinks, and J. D. Jorgensen, Phys. Rev. Lett. **87**, 047001 (2001).

[18] X. K. Chen, M. J. Konstantinovic, J. C. Irwin, D. D. Lawrie, and J. P. Franck, Phys. Rev. Lett. **87**, 157002 (2001).

[19] J. W. Quilty, S. Lee, A. Yamamoto, and S. Tajima, Phys. Rev. Lett. **88**, 087001 (2002).

[20] T. Takahashi, T. Sato, S. Souma, T. Muranaka, and J. Akimitsu, Phys. Rev. Lett. **86**, 4915 (2001).

[21] A. Brinkman, A. A. Golubov, H. Rogalla, O. V. Dolgov, J. Kortus, Y. Kong, O. Jepsen, and O. K. Andersen, Phys. Rev. B **65**, 180517(R) (2002).

[22] F. Bobba, D. Roditchev, R. Lamy, E-M. Choi, H-J. Kim, W. N. Kang, V. Ferrando, C. Ferdeghini, F. Giubileo, W. Sacks, S-I. Lee, J. Klein, and A. M. Cucolo, Supercond. Sci. Technol. **16**, 167 (2003).

[23] H. Suhl, B. T. Matthias, and L. R. Walker, Phys. Rev. Lett. **3**, 552 (1959).

[24] G. Binnig, A. Baratoff, H. E. Hoenig, and J. G. Bednorz, Phys. Rev. Lett. **45**, 1352 (1980).

[25] P. C. Canfield, P. L. Gammel, and D. J. Bishop, Phys. Today **51**(10), 40 (1998).

[26] A. Saito, A. Kawakami, H. Shimakage, H. Terai, and Z. Wang, J. Appl. Phys. **92**, 7369 (2002).

[27] H.-J. Tao, Z.-Z. Li, Y. Xuan, Z.-A. Ren, G.-C. Che, B.-R. Zhao, and Z.-X. Zhao, Physica C **386**, 569 (2003).

[28] H. Shimakage, K. Tsujimoto, Z. Wang, and M. Tonouchi, Appl. Phys. Lett. **86**, 072512 (2005).

[29] K. Ueda, S. Saito, K. Semba, T. Makimoto, and M. Naito, Appl. Phys. Lett. **86**, 172502 (2005).

[30] A. Barone and G. Paternó, *Physics and Applications of the Josephson Effect* (Wiley, New York, 1982).

[31] B. N. Taylor and E. Burstein, Phys. Rev. Lett. **10**, 14 (1963).

[32] I. K. Yanson, V. M. Svistunov, and I. M. Dmitrenko, Sov. Phys. JETP **21**, 650 (1965).

[33] A. Griffin and J. Demers, Phys. Rev. B **4**, 2202 (1971).

[34] P. Mukhopadhyay, J. Phys. F: Met. Phys. **5**, 903 (1979).

[35] C. J. Pethick and H. Smith, Ann. Phys. (N.Y.) **119**, 133 (1979).

[36] T. M. Klapwijk, G. E. Blonder, and M. Tinkham, Physica B & C **109–110**, 1657 (1982).

[37] M. Octavio, M. Tinkham, G. E. Blonder, and T. M. Klapwijk, Phys. Rev. B **27**, 6739 (1983).

[38] G. B. Arnold, J. Low Temp. Phys. **68**, 1 (1987).

[39] E. N. Bratus, V. S. Shumeiko, and G. Wendin, Phys. Rev. Lett. **74**, 2110 (1995).

[40] J. M. Rowell and W. L. Feldman, Phys. Rev. **172**, 393 (1968).

[41] L. J. Barnes, Phys. Rev. **184**, 434 (1969).

[42] M. A. Peshkin and R. A. Buhrman, Phys. Rev. B **28**, 161 (1983).

[43] N. van der Post, E. T. Peters, I. K. Yanson, and J. M. van Ruitenbeek, Phys. Rev. Lett. **73**, 2611 (1994).

[44] E. Scheer, P. Joyez, D. Esteve, C. Urbina, and M. H. Devoret, Phys. Rev. Lett. **78**, 3535 (1997).

[45] B. Ludoph, N. van der Post, E. N. Bratus, E. V. Bezuglyi, V. S. Shumeiko, G. Wendin, and J. M. van Ruitenbeek, Phys. Rev. B **61**, 8561 (2000).

[46] U. Zimmenrmann, S. Abens, D. Dikin, K. Keck, and V. M. Dmitriev, Z. Phys. B: Condens. Matter **97**, 59 (1995).

[47] M. Hurd, S. Datta, and P. F. Bagwell, Phys. Rev. B **54**, 6557 (1996).

[48] G. E. Blonder, M. Tinkham, and T. M. Klapwijk, Phys. Rev. B **25**, 4515 (1982).

[49] J. R. Schrieffer and J. W. Wilkins, Phys. Rev. Lett. **10**, 17 (1963).

[50] Yu. G. Naidyuk and I. K. Yanson, J. Phys.: Condens. Matter **10**, 8905 (1998).

[51] K. Gloos, Phys. Rev. Lett. **85**, 5257 (2000).

[52] N. Miyakawa, P. Guptasarma, J. F. Zasadzinski, D. G. Hinks, and K. E. Gray, Phys. Rev. Lett. **80**, 157 (1998).

[53] R. C. Dynes, V. Narayanamurti, and J. P. Garno, Phys. Rev. Lett. **41**, 1509 (1978).

[54] G. J. Strijkers, Y. Ji, F. Y. Yang, C. L. Chien, and J. M. Byers, Phys. Rev. B **63**, 104510 (2001).

[55] L. Shan, H. J. Tao, H. Gao, Z. Z. Li, Z. A. Ren, G. C. Che, and H. H. Wen, Phys. Rev. B **68**, 144510 (2003).

[56] P. A. Lee, J. Appl. Phys. **42**, 325 (1971).

[57] S. Piano, F. Bobba, F. Giubileo, A. Vecchione, and A. M. Cucolo, J. Phys. Chem. Solids (in press).

[58] S. Piano, F. Bobba, F. Giubileo, A. Vecchione, M. Gombos, and A. M. Cucolo, cond-mat/0509346 (unpublished).

[59] Ya. G. Ponomarev, S. A. Kuzmichev, M. G. Mikheev, M. V. Sudakova, S. N. Tchesnokov, N. Z. Timergaleev, A. V. Yarigin, E. G. Maksimov, S. I. Krasnosvobodtsev, A. V. Varlashkin, M. A-Hein, G. Müller, H. Piel, L. G. Sevastyanova, O. V. Kravchenko, K. P. Burdina, and B. M. Bulychev, Solid State Commun. **129**, 85 (2004).